

© 2017 IEEE. Personal use of this material is permitted. Permission from IEEE must be obtained for all other uses, in any current or future media, including reprinting/republishing this material for advertising or promotional purposes, creating new collective works, for resale or redistribution to servers or lists, or reuse of any copyrighted component of this work in other works.

A 36 GHz HTS MMIC Josephson Mixer – Simulation and Measurement

Ting Zhang, Xiang Gao, Wei Wang, Jia Du, Colin Pegrum, Yingjie Jay Guo, *Fellow, IEEE*

Abstract—Modelling, simulation and measurement of a compact 36 GHz high-temperature superconducting (HTS) monolithic Josephson junction mixer are presented in this paper. A full HTS MMIC (microwave monolithic integrated circuit) simulation was carried out for the circuit combining HTS passive devices and the Josephson junction. Optimal impedance matching and bias condition were investigated, and the circuit layout was designed accordingly. The HTS circuit has a compact dimension of $5 \times 4 \times 0.3 \text{ mm}^3$, including filters, resonators and impedance matching circuits. The HTS MMIC mixer was fabricated and packaged with a LNA to realize a receiver front-end with a total dimension of $28 \times 25 \times 15 \text{ mm}^3$. Measurement result showed an overall conversion gain around 35 dB, with LO driving power around -45 dBm at operating temperature of 40 K.

Index Terms— High temperature superconductor (HTS), MMIC, Josephson junction, mixer, simulation, receiver front-end.

I. INTRODUCTION

High temperature superconducting (HTS) materials have ultra-low surface resistance at frequencies below 100 GHz, which has been applied to make filters and resonators with superior performance [1-3]. The low-noise and high non-linearity properties of the HTS Josephson junctions make them ideal for the key component of mixers [4-6]. With HTS passive and active devices integrated monolithically, HTS MMIC Josephson mixers have been developed at different frequencies, showing features of compactness, low loss and low power consumption [7-9]. The performance of the MMIC Josephson mixer can be further improved with proper impedance matching between the junction and HTS filters. Recently, modelling of HTS MMIC Josephson mixer has been reported, in which the optimal impedance matching was investigated [10]. The modeling has provided a theoretical guidance for HTS MMIC mixer design to achieve a better RF coupling and a higher conversion gain.

In this paper, a 34 -38 GHz HTS MMIC Josephson mixer is designed, simulated and measured. A Verilog-A model of a Josephson junction is established and imported into the system

Ting Zhang is with CSIRO Data61, Marsfield, NSW 1710, Australia (e-mail: Ting.Zhang@csiro.au).

Xiang Gao is with CSIRO Manufacturing, Lindfield, NSW 2070, Australia (e-mail: Xiang.Gao@csiro.au).

Wei Wang is with SIMIT CAS, Shanghai 20050, China.

Jia Du is with CSIRO Manufacturing, Lindfield, NSW 2070, Australia (e-mail: Jia.Du@csiro.au).

Colin Pegrum is with the Department of Physics, University of Strathclyde, Glasgow G4 0NG, UK (e-mail: colin.pegrum@strath.ac.uk).

Yingjie Jay Guo is with University of Technology, Sydney, NSW 2007, Australia (e-mail: Jay.Guo@uts.edu.au).

simulator to realize a full HTS MMIC circuit simulation containing the HTS passive circuit models. Impedance matching optimization between the junction and RF input port is investigated. Bandpass and lowpass filters are designed for RF and IF ports based on simulation results, as well as a compact dual-stub impedance matching circuit to improve the RF coupling efficiency. The HTS MMIC Josephson mixer was packaged with a semiconductor LNA to realize a receiver front-end. Design considerations, simulation results of filters and the MMIC mixer, along with experimental results of the integrated HTS front-end, including conversion gain, bias condition and dynamic range, are reported.

II. MODELING AND SIMULATION OF THE HTS MMIC JOSEPHSON MIXER

Fig. 1 shows the schematic of the 36 GHz MMIC Josephson mixer simulation model. The simulation was carried out using Keysight Advanced Design System (ADS) with an imported Verilog-A model of a Josephson junction. We omitted the junction resistance from the Verilog-A model and used a separate shunt resistor across the junction with resistance R_n instead. In this way we can include thermal noise in the time-domain simulation, which is critical to the simulation accuracy. Detailed simulation approach of the HTS MMIC mixer has been described in [10]. The junction critical current I_c and intrinsic resistance R_n were set to $420 \mu\text{A}$ and 5Ω , which were the junction characteristics in the MMIC mixer. The bandpass filter was set to have a passband from 34 to 38 GHz, and an adjustable output impedance Z_{RF} ; operation frequency of the LO resonator was set to 36 GHz with a 400 MHz bandwidth; the lowpass filter's cutoff frequency was set to be 25 GHz. Due to the addition of the filtering networks, the impedance matching between the junction and RF port can

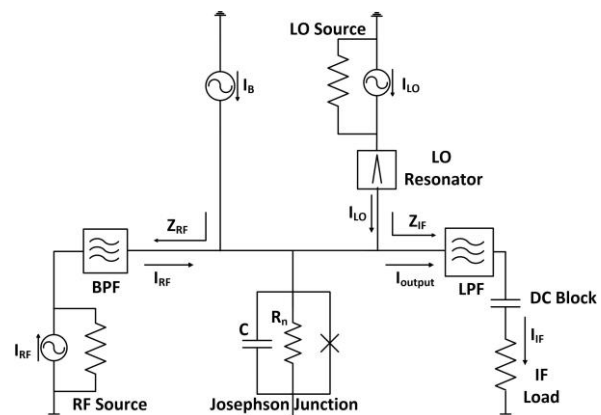


Fig. 1. Schematic of the HTS MMIC Josephson mixer.

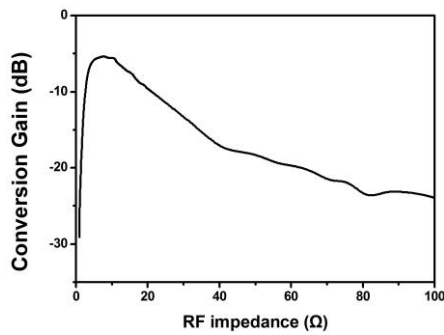


Fig. 2. Simulated conversion gain of the MMIC mixer as a function of the RF input impedance.

be analyzed independently without being affected by other load impedances. A parameter sweep of conversion gain was carried out against Z_{RF} to investigate the optimal RF impedance matching, and the result is shown in Fig. 2. The maximum conversion gain of -5 dB occurs when Z_{RF} is matched to R_n . The simulation result can be explained using the circuit model in Fig. 1, where the RF impedance is supposed to match to junction impedance R_n to achieve minimum insertion loss.

DC I-V behavior, LO and DC current bias conditions and dynamic range of the HTS MMIC Josephson mixer were simulated after the RF impedance had been optimized. Simulation results are displayed and compared with measurement ones in Section V.

III. MONOLITHIC HTS JOSEPHSON MIXER CONFIGURATION

Fig. 3 shows the layout of the HTS monolithic Josephson mixer chip. The RF and LO ports were designed to be separated by the Josephson junction. The two DC lines are of $\frac{3}{4}$ wavelength at 36 GHz. The left pad was grounded with bonding wires during packaging to provide a ground for the junction at IF frequency, while the right pad was connected to high-impedance components to form an open end and hence a grounding for the junction at RF frequency. Bandpass and lowpass filters were introduced for the RF and IF ports to improve the coupling efficiency to the mixer and to isolate input and output signals. A typical H-shaped half-wavelength resonator was applied to the LO input port, with a resonance frequency at 36 GHz and a 3-dB bandwidth of 400 MHz. The proposed bandpass filter consists of two dual-mode resonators, and a cross-coupling is introduced between the odd mode of the two resonators to produce a pair of transmission zeros outside the passband. Therefore, a better RF signal selectivity

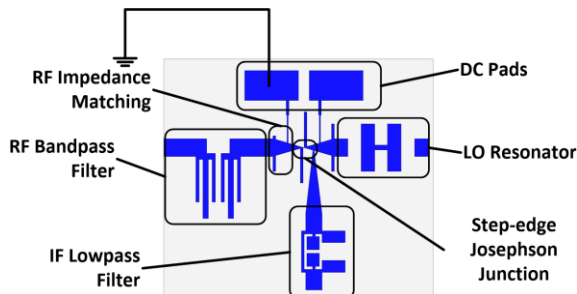
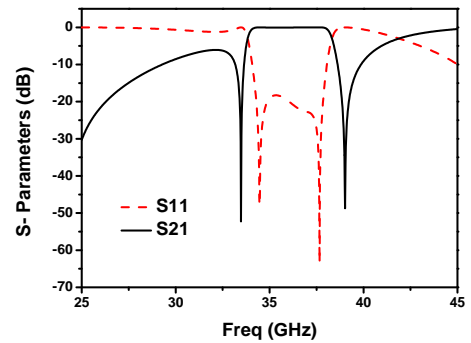
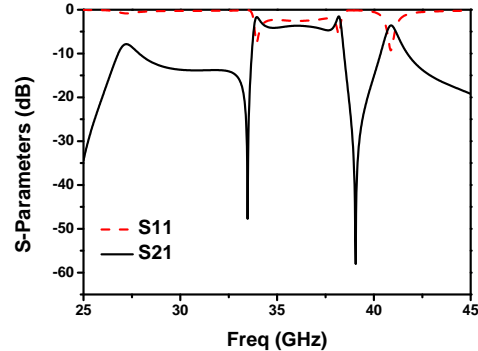


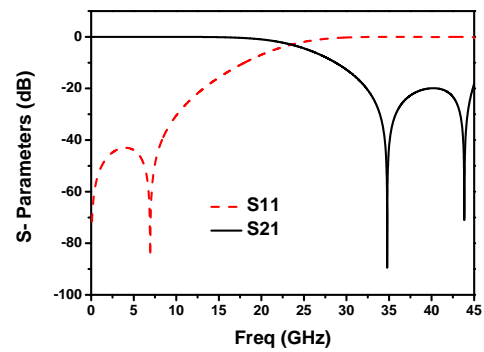
Fig. 3. Photograph of the HTS monolithic Josephson mixer.



(a)



(b)



(c)

Fig. 4. Simulation result of (a) the bandpass filter with both 50 terminals, (b) the bandpass filter terminated with 50 Ω and 5 Ω impedance, and (c) the lowpass filter with 50 Ω terminals.

of transmission response is achieved. Simulation result of the bandpass filter in Fig. 4 (a) shows that the filter has a passband from 34 GHz to 38 GHz, and two transmission zeros are observed at 33.5 GHz and 38.5 GHz. A dual-stub structure was applied to the tapered connection line between the RF filter and the junction, to improve the impedance matching between the junction normal resistance R_n and RF filter. Fig.4 (b) shows the simulated S-parameters between the RF input port to the junction, with an insertion loss around 3.5 dB within the desired bandwidth. The lowpass filter was designed based on a typical L-C element circuit, with a cross-coupling introduced between the two pads in the middle, to create a transmission zero point in the filter’s stopband. In this way a wider stopband is achieved, with S21 below -20 dB from 32 GHz to 45 GHz, as shown in Fig. 4 (c). High impedance quarter-wavelength transmission lines are used for the Josephson junction DC biasing to prevent RF interference.

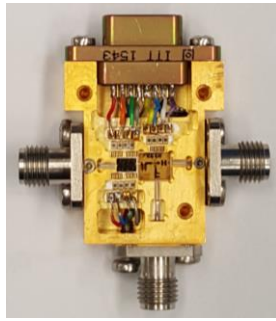


Fig.5. Photograph of packaged HTS receiver front-end module.

All the passive and active devices were integrated onto a $5 \times 4 \times 0.3 \text{ mm}^3$ MgO substrate with a dielectric constant of 9.7. The compactness of the mixer has been significantly improved, compared with our previous work at 31.5 GHz, which has an overall dimension of $10 \times 10 \times 0.5 \text{ mm}^3$ [9]. Cavity resonance, which brought in extra insertion loss in previous design, has also been prevented due to the reduction of the circuit chip size.

IV. FABRICATION AND MEASUREMENT DETAILS

The mixer was fabricated on a single-sided $\text{YBa}_2\text{Cu}_3\text{O}_{7-x}$ (YBCO) film on MgO substrate using the CSIRO developed step-edge junction technology [11]. More detailed description of the device fabrication procedures and measurement set-up can be found in earlier papers [7-9]. The fabricated mixer was packaged together with an OMMIC LNA chip and other lumped element circuits into a thermal-conducting copper housing with Au coating as shown in Fig. 5. Silver epoxy was used to make the connections of the filter to the K connectors

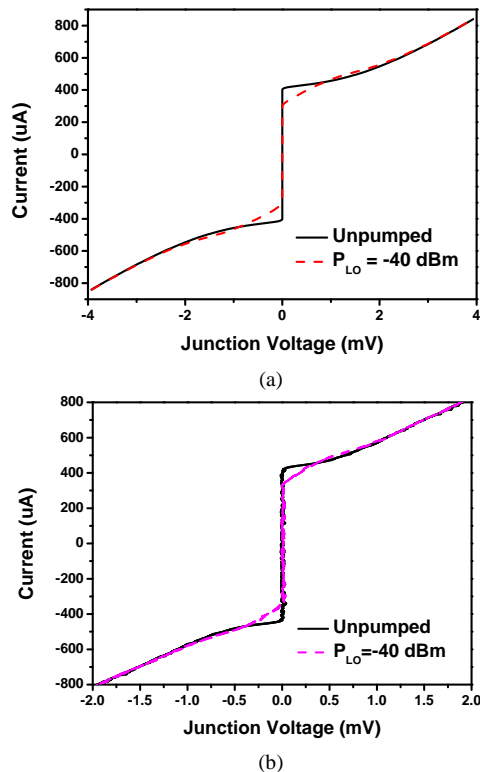


Fig. 6. (a) Simulated DC I-V curve of the Josephson junction and (b) the measurement result.

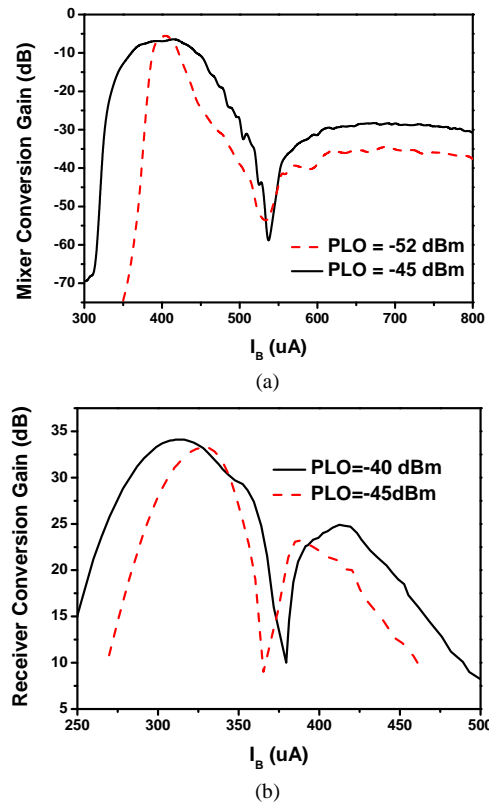


Fig. 7. (a) Simulated conversion gain vs DC bias current and (b) its measurement result.

and ground the substrate to the housing base plate. The packaged module was then cooled down to an operating temperature in 20 - 77 K with a commercial 2-stage pulse-tube cryocooler. DC current sources were used to bias the Josephson device and the MMIC LNA. The microwave RF signal generated by an Anritsu 68087C Synthesized CW Generator was applied to the RF port. An Agilent E4407B spectrum analyzer was connected to the IF port for output power measurement.

V. RESULTS COMPARISON AND DISCUSSION

Full evaluation of the HTS receiver front-end has been carried out at temperatures from 20 to 77 K. For clarity, only the results of at 40 K are presented and compared with simulated results of the HTS mixer. The performance of the HTS mixer cannot be characterized due to its integration with the LNA chip, which has not been measured at cryogenic temperatures. Therefore, measurement results of the whole HTS receiver are presented for a qualitative comparison with simulation results. Fig. 6 shows the simulated and measured I-V suppression behavior of the step-edge junction. A good consistency is observed between the simulation and measurement results. Unsuppressed junction critical current I_{c0} is around $425 \mu\text{A}$, and is suppressed down to $300 \mu\text{A}$ by a LO signal of -40 dBm . The junction normal resistance R_n , determined from the linear section of the I-V curve, is about 5Ω . The $I_{c0} R_n$ product obtained for this junction is over 2 mV , which is a high value.

Comparison of conversion gain as a function of DC bias

current I_B is made between simulation and measurement as shown in Fig. 7 (a) and (b). The double-peak behavior, which has been explained in [12], is clearly observed in both results, as well as the feature that a lower LO driving power will result in a narrower operation range. Instead of battery-driven instruments used for DC I-V measurement, AC power-supplied voltage meter was applied to monitor the voltage of the junction and then to extract the bias current, which brought extra noise and interferences to the junction and affected its critical current. This explains the inconsistency occurred in Fig. 6 (b) and Fig. 7 (b), where the critical current pumped by -40 dBm LO signal were different. Other than the issue explained above, the measurement results agree qualitatively well with the simulation. Simulated and measured LO dependence of conversion gain is shown in Fig. 8, where a qualitative agreement of the shape of the single peak traces is observed. The optimal LO power is between -45 to -40 dBm, much lower than the requirement for pumping a semiconductor mixer, which is a major advantage of the Josephson mixer. Simulated DC and LO driving condition indicate an optimal conversion gain of -5 dB for the MMIC mixer, while the measured HTS receiver front-end shows an optimized gain at 35 dB. Fig. 9 (a) shows the simulation result of the HTS mixer's linearity performance, where a 1 dB gain compression point at -75 dBm is observed. Measured dynamic range of the receiver front-end is shown in Fig. 9 (b), indicating a 1 dB gain compression point around -89 dBm and a RF input range from -135 dBm to -95 dBm without compression.

All the measurement results have shown a good qualitative agreement with simulation ones overall, except for the

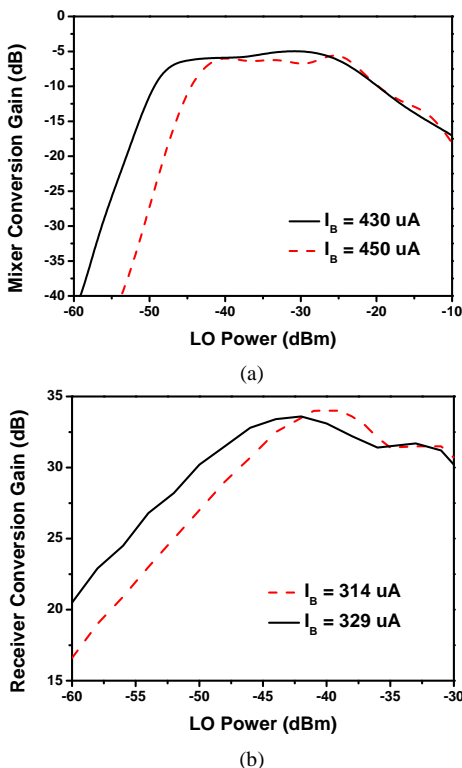


Fig. 8. (a) Simulated conversion gain vs LO power and (b) its measurement result.

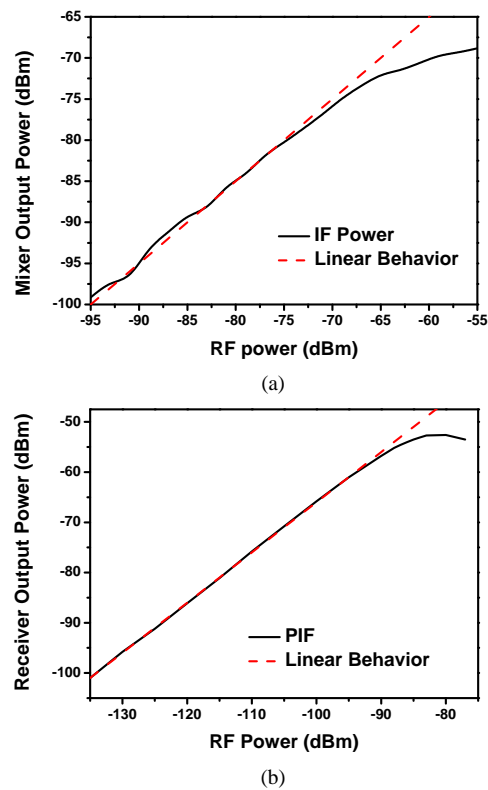


Fig. 9. (a) Simulated IF output power versus RF input power, and (b) the receiver's measurement result.

difference in absolute values, which is due to the inclusion of LNA and the extra loss introduced by cables, transmission lines and filter not been included in the simulation.

VI. CONCLUSION

In this paper, we have presented the simulation and measurement results of a compact Ka band HTS MMIC Josephson mixer. An HTS Josephson junction was modeled and simulated together with passive devices for optimal impedance matching. Compact, high performance HTS bandpass and lowpass filters were designed and integrated monolithically with the Josephson junction on a single MgO substrate, achieving a compact functioning full front-end receiver. Measurement results show a qualitative agreement with the simulation, with a conversion gain around 35 dB for the presented receiver front-end at 40 K. Such performance and compactness feature demonstrated the potential of the HTS front-end receiver technology for Ka band high-sensitivity detections.

ACKNOWLEDGMENT

We gratefully acknowledge technical assistance from Mei Shen and Henry Kanoniuk for packing and wire bonding and Ms Jeina Lazar for HTS chip fabrication.

REFERENCES

- [1] M. Klauda et al., "Superconductor and cryogenics for future communication systems," *IEEE Trans. Microwave Theory Tech.*, vol. 48, pp. 1227–1239, Jul. 2000.

- [2] R. R. Mansour, "Microwave superconductivity," *IEEE Trans. Microw. Theory Techn.*, vol. 50, pp. 750-759, 2002.
- [3] R. W. Simon, R. B. Hammond, S. J. Berkowitz, and B. A. Willemsen, "Superconducting microwave filter systems for cellular telephone base stations," *Proc. IEEE*, vol. 92, pp. 1585-1596, 2004.
- [4] D. P. Butler, W. Y. Yang, J. Wang, A. Bhandari, and Z. Celik-Butler, "Conversion loss of a YBa₂Cu₃O₇ grain boundary mixer at 20 GHz," *Appl. Phys. Lett.*, vol. 61, p. 20, Jul. 1992.
- [5] Y. Taur, J. Claassen, and P. Richards, "Josephson junctions as heterodyne detectors," *IEEE Trans. Microw. Theory Techn.*, vol. 22, no. 12, pp. 1005-1009, Dec. 1974.
- [6] M. Malnou, C. Feuillet-Palma, C. Ulysse, G. Faini, P. Febvre, M. Sirena, L. Olanier, J. Lesueur, and N. Bergeal, "High-Tc superconducting Josephson mixers for terahertz heterodyne detection," *J. Appl. Phys.*, vol. 116, no. 7, p. 074505, 2014.
- [7] J. Du, T. Zhang, Y. J. Guo, and X. W. Sun, "A high-temperature superconducting monolithic microwave integrated Josephson down-converter with high conversion efficiency", *Appl. Phys. Lett.* vol. 102, 212602, 2013.
- [8] J. Du, D. D. Bai, T. Zhang, Y. Jay Guo, Y. S. He and C. M. Pegrum, "Optimised conversion efficiency of a HTS MMIC Josephson down-converter", *Supercond. Sci. Technol.*, vol. 27, p. 105002, 2014.
- [9] T. Zhang, J. Du, J. Wang, D. D. Bai, Y. Jay Guo, and Y. S. He, "30 GHz HTS receiver front-end based on monolithic Josephson mixer", *IEEE Trans Appl. Supercond.*, vol. 25, No. 3, p. 140065, 2015.
- [10] T. Zhang, C. Pegrum, J. Du, Y. J. Guo, "Simulation and measurement of a Ka-band HTS MMIC Josephson junction mixer," submitted to *Supercond. Sci. Technol.*
- [11] C. P. Foley, et al., "Fabrication and characterisation of YBCO single grain boundary step edge junctions," *IEEE Trans. Appl. Supercond.*, vol. 9, pp. 4281-4284, 1999.
- [12] C. Vanneste, et al., "I-V characteristics of microwave-driven Josephson junctions in the low-frequency and high-damping regime", *Phys. Rev. B*, vol. 31, pp. 4230 - 4233, Apr. 1985.